Characterization of Earth observing satellite instruments for response to spectrally and spatially variable scenes

S. W. Brown[1], B. Myers[1,2], R. A. Barnes[3], J. P. Rice[1*]

[1]National Institute of Standards and Technology, Gaithersburg, MD, USA 20899
[2]Summer Undergraduate Research Fellow, Appalachian State University, Boone, NC 28608
[3]Science Applications International Corporation, Beltsville, MD 20705

ABSTRACT

Earth-observing satellite sensors are calibrated in the laboratory against blackbody and lamp-based uniform optical radiation standards. These sources and additional characterization tests fail to approximate the spatially, spectrally, and temporally complex scenes viewed on-orbit by these sensors. The lack of appropriate diagnostic tools limits the ability of researchers to fully characterize and understand the radiometric performance of sensors before deployment. The consequences of these limitations are that problems in a sensor's performance, e.g. optical crosstalk, scattered light, earth-shine, are often first observed on-orbit. Advanced radiometric characterization artifacts, able to produce realistic spectral distributions and spatial scenes in the laboratory, would enable more complete instrument characterization, with the resulting potential benefit of improved on-orbit performance.

In this work, we present a radiometric platform for the development of application-specific metrics to quantify the performance of sensors and systems viewing realistic spectral and spatial scenes. There are two components to the platform, both based on Digital Micromirror Device (DMD) technology. The first component is a spectrally programmable light source. This source can reproduce, with high fidelity, the spectral distributions of targets observed on-orbit, for example, the water-leaving radiances for various phytoplankton chlorophyll-*a* concentrations and atmospheric conditions. The second component is a spatially programmable projection system. This system uses the programmable spectral distributions from the light source as basis functions to generate complex spatial scenes with true spectral content. Using this platform, sensor and system performance may be quantified in terms of the accuracy of measurements of standardized sets of complex source distributions. In essence, the programmable source will be a radiometric platform for advanced sensor characterization, enabling a pre-flight validation of the pre-flight calibration. The same platform can also serve as a basis for algorithm testing and instrument comparison. With the same fundamental technology, platforms can be developed to cover the full reflected solar region; similar platforms can in principle be developed for the thermal IR region as well.

Keywords: Calibration, characterization, hyperspectral, imaging, spectroscopy, radiometry, remote sensing

1. INTRODUCTION

Ideally, remote sensing satellite sensor performance is validated using a source with radiometric characteristics similar to those that will be seen on-orbit. Simpler source distributions are useful for the radiometric characterization of sensors. For multi-band instruments with multiple detectors per band, artifacts within the focal plane are a principal concern in instrument performance. For example optical crosstalk, the contamination of the measurement in one band by light scattered from another band, is a well-known artifact [1]. Testing for crosstalk has been done by viewing slits of varying width, generally slits illuminated by quartz halogen lamps. In some cases, filters over the slits have been used to better approximate the spectral shape of the Earth-exiting radiance [2]. A simple set of test scenes of narrow stripes of light of varying color in the along track direction of instrument onboard the spacecraft is ideal to test for crosstalk, as is a set of similar scenes in the cross track direction. This can be done using a monochromator with variable slit widths as a light source. However, changes in the slit widths can be cumbersome and optical considerations may require curved slits to maintain a monochromatic exit beam. In addition, the flux level from monochromator-based light sources is generally low. Simple external scenes with stripes of different widths, flux levels, colors, and orientations can provide a much improved diagnostic test of crosstalk within a focal plane.

Simple, unambiguous test scenes can be central to the pre-launch testing of artifacts in Earth-observing satellite instruments. For example, stray light contamination in a scene due to a finite point-spread response (spatial out-of-field

Earth Observing Systems XII, edited by James J. Butler, Jack Xiong,
Proc. of SPIE Vol. 6677, 667705, (2007) · 0277-786X/07/$18 · doi: 10.1117/12.731765

stray light) is a common problem in remote sensing ocean color instruments. A simple scene consisting of dark and extended cloud-like sections can provide a test for spatial out-of-field stray light. For diagnostic purposes, the scene can have sharp bright-to-dark transitions. For additional testing, the scenes can mimic the gradual transition of light intensity at the edges of clouds. By adding control over the spectral composition of a scene, instrument response to the bright-to-dark transition at a coast line can also be diagnosed and tested.

More complex test scenes, representative of those observed on-orbit, can be used to validate the radiometric characterization and calibration of sensors in the laboratory. More efficient utilization of resources can be achieved by combining individual test, characterization, and calibration procedures that are required for a thorough understanding of a sensor's performance into procedures that utilize these advanced radiometric platforms.

In this work, we discuss a fully integrated radiometric characterization and calibration platform called a Hyperspectral Image Projector (HIP) that would have the capability of generating standardized sets of spatially complex scenes with high spectral fidelity [3-6]. In Section 2, we describe the components of the HIP system, a Spectrally Tunable Source, capable of generating complex spectral distributions, and a spatial projection system. In Section 3, we describe the realized bench-top HIP system.

2. HYPERSPECTRAL IMAGE PROJECTOR (HIP)

Hyperspectral Image Projectors (HIP), based on Digital Light Processing (DLP) [7] micromirror array technology, project dynamic 2-dimensional (2D) hyperspectral scenes in the visible through the short-wave infrared for the characterization, calibration, and validation of multi-spectral and hyperspectral imagers. With the HIP, spatially structured scenes of known spectral radiance are projected into the unit-under-test (UUT) through a collimator, and the measured spectral radiance in every pixel is compared with the projected value. In its most general form, the HIP projects different arbitrarily programmable spectra into each spatial pixel of a 2D image [4-6]. The projected scenes can be either computer-generated using a radiative transfer model coupled to a signature database or derived from actual field measurements. The HIP enables assessment of sensor performance for a defined set of land and ocean compositions and varying atmospheric conditions expected to be viewed by the sensor on-orbit.

The projected radiances are determined using a calibrated reference imager viewing the same scene. The reference imager will be characterized on the NIST facility for Spectral Irradiance and Radiance responsivity Calibrations using Uniform Sources (SIRCUS) [8] and images corrected for both spectral [9] and spatial scattered light [10].

The HIP is schematically illustrated Fig. 1. It consists of a spectral engine coupled to a spatial engine. The spectral engine [11] produces a series of programmable spectra, which we call basis spectra. These could be, for example, the endmember spectra (e.g., spectra of the composite materials) of a real hyperspectral image that is to be projected, or simply Gaussian-like spectral distributions with different center wavelengths. The spatial engine projects the basis spectra, in the correct proportions in each spectral region, sequentially to create a time-averaged spatially complex scene with realistic spectral content. In the following we first describe the spectral engine and spatial engines separately, then in combination.

The spectral engine

The spectral engine works as follows. Light from a broadband source is fiber-coupled into the spectral engine through an entrance slit (not shown in the figure). The light is collimated by mirror M1 and reflected onto Prism1. The spectrally dispersed output of Prism1 is imaged by mirror M2 onto a digital micromirror device (DMD). This is an array of mirrors having, for example, 1024 columns and 768 rows. This portion of the spectral engine is identical in concept and design to a conventional spectrograph, with the DMD replacing a standard two-dimensional charge-coupled device (CCD) detector array. As in a spectrograph, an image of the entrance slit is formed on the DMD array, with a particular incident wavelength imaged onto a specific columnar region. Thus, each of the DMD columns in Fig. 1 reflects a different center wavelength with a spectral bandwidth λ_1 to λ_2 determined by the dispersion of the prism.

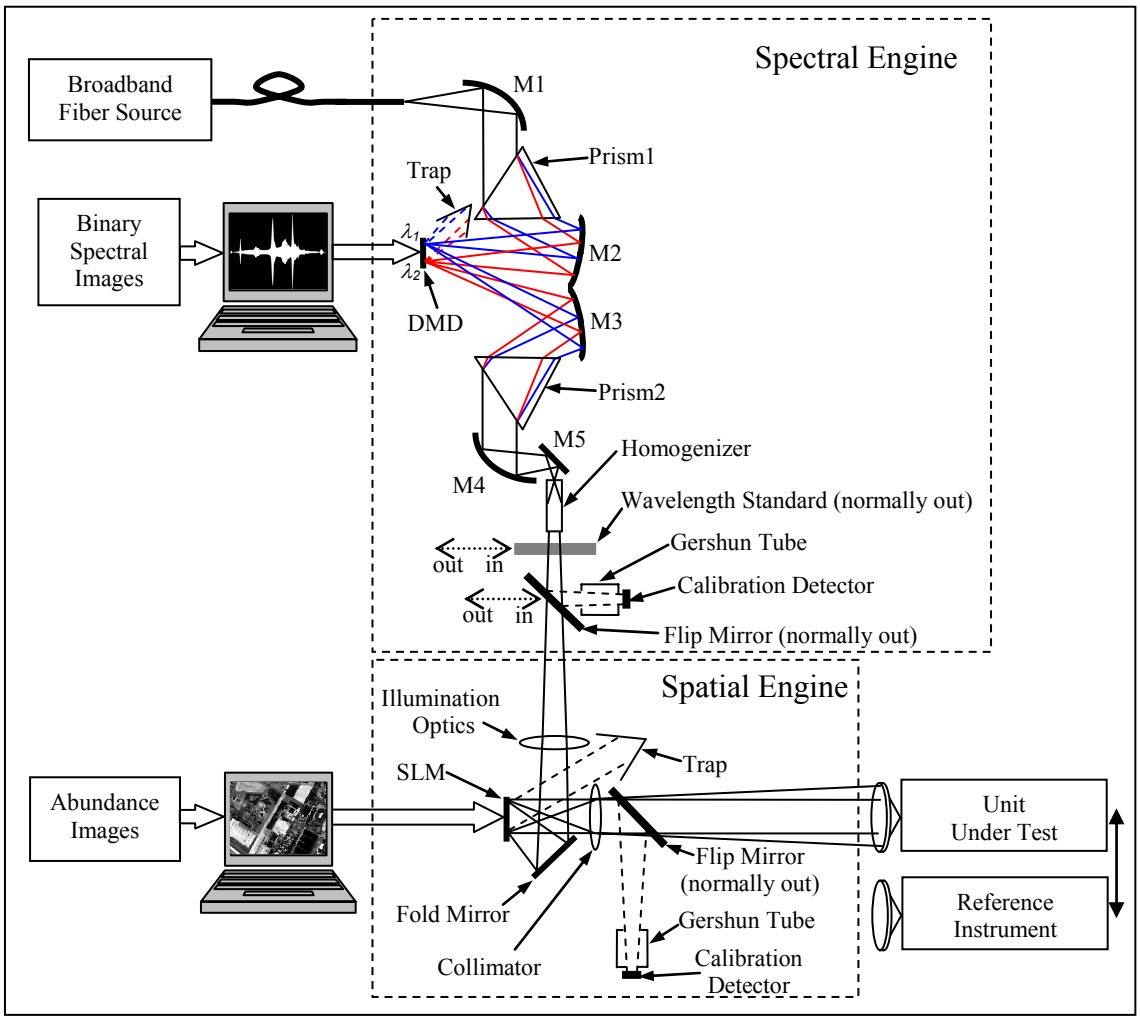

Figure 1. Schematic of the Hyperspectral Image Projector (HIP) concept. The series of endmember spectra produced by the spectral engine illuminate the spatial engine, which synchronously projects the corresponding abundance images into the Unit Under Test (UUT). The DMD and SLM are shown edge-on in this schematic. The full set of endmember spectra and corresponding abundance images are displayed within the integration time of the UUT, which then measures the projected hyperspectral scene. Truth data comes from an on-board calibrator, consisting of a wavelength standard and calibration detector. The on-board calibrator has a scale transferred from the NIST Reference Instrument, which alternately views the same scene as the UUT during calibration of HIP at NIST.

A binary spectral image sent to the DMD from the computer determines which DMD micromirrors are "on" and which are "off." "On" micromirrors are tilted clockwise (+12° about the micromirror diagonal) from the DMD normal; "Off" micromirrors are tilted counterclockwise (–12° about the micromirror diagonal) from the DMD. On mirrors reflect the light towards mirror M3 while off mirrors reflect the light into a beam trap. Mirror M3 collects the light from the on-state DMD micromirrors and collimates it onto Prism2. This prism is oriented such that spectrally dispersed light is re-combined spatially, as in a double subtractive spectrograph. Mirrors M4 and M5 focus the output of the spectral engine to a circular spot having a diameter of about 5 mm and feed it into a beam homogenizer. This is long rectangular tube with open ends having walls made from four flat specular mirrors. Through multiple internal reflections from these highly reflective walls, the circular, spatially non-uniform input beam is reshaped into a spatially uniform output beam having a rectangular cross section that matches that of the spatial light modulator (SLM) of the spatial engine. During normal projection operations, the output beam of the homogenizer is sent directly into the spatial engine.

To a first order approximation, the fraction of the 768 micromirrors in each DMD column that are "on" determines the relative spectral intensity at the wavelength corresponding to that column reflected onto mirror M3. Thus, at any instant in time, the spectral engine can generate an arbitrary spectrum, such as a member of a set of endmember spectra derived from a desired hyperspectral scene, within the spectral range of the spectrograph and with the resolution determined by the spectrograph design. The spectral engine can cycle through spectra at rates up to 16 kHz, which is the binary image update rate of the DMD.

The wavelength standard and calibration detector shown in the spectral engine of Fig. 1 are used during calibration operations. These are automated operations that typically take on the order of 30 s or less. If a calibrated, stable detector is used, the source can be calibrated absolutely against the reference detector. Si detectors covering the 350 nm to 1100 nm spectral window have been shown to be stable over years. Similar results have been obtained for InGaAs detectors covering the 900 nm to 1.7 μm spectral range. Thus the calibration can in principle be maintained in the field for lengthy periods. Independent of the spatial engine, the absolute, detector-based spectral engine, able to generate arbitrary, user-defined spectral distributions, represents a significant advance over conventional calibration sources, which have limited spectral distributions and must be sent back to a calibration laboratory routinely for re-calibration. In its most basic design, the spectral engine can accept any fiber-optically coupled input source, and the output can be sent to a fiber bundle or light guide. It is meant to be rack-mountable. Its design is similar to the Newport Corporation's discontinued Lambda Commander product, developed as a programmable source to support the telecommunications industry [12].

The Lambda Commander used Amplified Spontaneous Emission (ASE) sources in the 1400 nm to 1600 nm spectral range. We envision expanding the spectral coverage using newly developed supercontinuum (SC) sources [13]. These sources have several mW/nm of spectral radiant power density and currently cover the spectral range from 450 nm to 2500 nm. To date, emission from SC sources has been demonstrated down to approximately 350 nm. The spectral power distribution from a commercial SC source is shown in Fig. 2 [13]. In these sources, the light is generated in a single mode, 'holey' fiber with a core diameter of approximately 5 μm. While the light is often subsequently coupled into a larger core diameter light guide, inputting the light from the single mode fiber directly into the spectral engine would correspond to the spectral engine having a 5 μm wide entrance slit. The entrance slit width is one of the determining elements in a spectrograph's spectral resolution, with narrower slit widths corresponding to higher spectral resolution. However, for typical extended area sources, reducing the entrance slit width concurrently reduces the amount of incident flux incident on the DMD. For the SC, in principle, none of the incident flux is lost as the slit is narrowed down to 5 μm, meaning the SC-based light engine can have both high radiant flux and high spectral resolution.

The spatial engine

The spatial engine works as follows. The light from the spectral engine is passed through the spatial engine illumination optics, which serves to provide spatially uniform illumination of the spatial light modulator (SLM) (Fig. 1). The SLM can be a DMD, a liquid crystal on silicon (LCOS) array, or any other suitable transmissive or reflective high-resolution spatial light modulator that can display the grey scale abundance image. We are currently using DMDs as the spatial engine SLM, but LCOS arrays could replace the DMDs. The 2D spatial image displayed on the SLM is at the focus of a collimator that fills the entrance pupil of the UUT and, alternately, the reference instrument. Unwanted spatial light from the SLM is captured by the spatial engine trap. Contrast ratio is an important consideration in the spatial projection system. Spatially scattered light, originating for example from the edges of the mirrors in the DMD, in a scene reduces the bright-to-dark contrast and can potentially limit the capability of these systems to characterize the response of satellite sensors to complex scenes. Contrast ratios of 7500:1, currently available in commercial DMD projection systems [14], should be sufficient for testing purposes.

The flip mirror, Gershun tube, and calibration detector are used only for calibration. The calibration detector could in principle be a large area single element detector, or a 2-d array detector (e.g. a CCD). The calibration detector is calibrated by the reference instrument at some point, and is then expected to maintain the scale for some period of time, to be determined empirically.

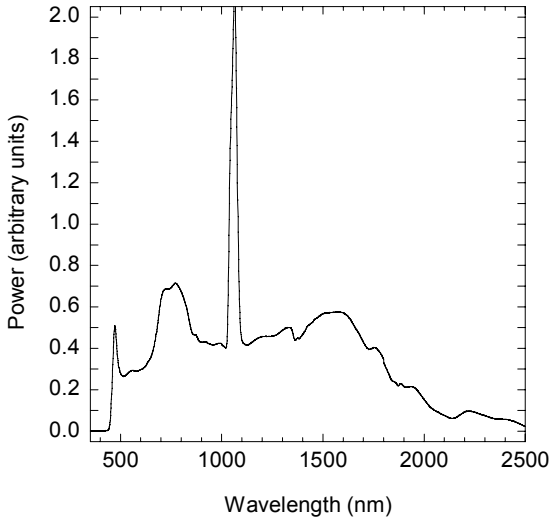

Figure 2. Output spectrum from a supercontinuum source [13].

The full 2D HIP works as follows. The spectral engine DMD and the spatial engine SLM both display their respective images in sync with a trigger pulse. Successive pulses trigger the production of the successive endmember spectra on the spectral engine and the corresponding abundance images on the spatial engine. The trigger is derived from the UUT so as to synchronize frame rates to avoid temporal aliasing. The complete set of endmember spectra and associated abundance images are displayed within the integration time of the UUT. Alternately, each member of the set is synchronously captured as a separate UUT frame and the frames are co-added in software.

Consider, as a simple example, a multi-spectral or hyperspectral UUT based upon a 2D staring focal plane array, with 1:1 mapping of HIP spatial pixels to UUT pixels, and consider the ideal situation in which aberrations, scattered light, air transmittance, and other contaminating effects are ignored. During its integration time, each pixel of this UUT is exposed to all endmember spectra in proportion to the corresponding levels coded for that pixel in the abundance images. Any pixel's temporally-integrated spectrum is then a linear combination of the endmember spectra. The counts from any spatial pixel of the UUT collected during the integration time then represent the radiance from the real scene from which the endmember spectra and abundance images were derived. While there are, in reality, several contaminating effects to be properly dealt with, to first order the HIP is indeed capable of simulating reality in that every pixel of a projected 2D image can have any spectrum. In addition, many of these effects, present in a real image, are properly accounted for with the reference instrument if they are stable.

Fig. 1 is merely a schematic representation of the concept. Any of the optics in Fig. 1 may of course be lenses instead of mirrors, and the dispersing elements may be transmissive or reflective gratings instead of prisms. The illumination and collimation optics in the spatial engine will be specially designed reflective or refractive subsystems, rather than single element lenses as drawn in the schematic. Multi-chip (up to 6 DMD elements) cinematic projection systems are commercially available. Utilization of multi-chip strategies improves the available power available for a given set of basis spectra, because we are using a time-division multiplexing scheme to produce the hyperspectral image.

3. REALIZATION OF BENCH-TOP HIP

A bench-top HIP has been realized [6]. The layout is shown in Figure 3, with the red solid line showing the optical path. Figure 4 shows an image of the earth projected onto a screen, with the reference camera in the foreground. In Ref. 6, we introduced the concept of using the Sequential Maximum Angle Convex Cone (SMACC) algorithm for automatic dimensional reduction to prepare real data cubes for projection with HIP in broadband mode, and provided a detailed example, including spectrally matching the endmember spectra. We have demonstrated the prototype HIP for projection of three spectral planes, such as standard RGB images.

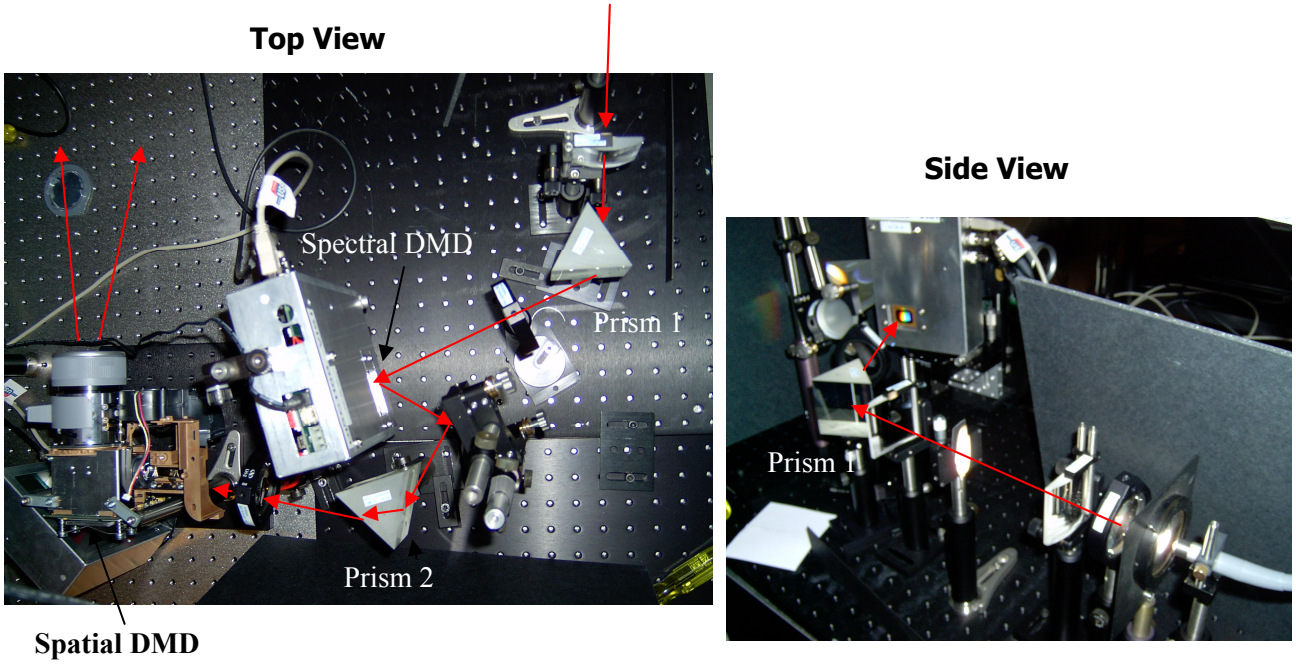

Figure 3. Layout of the breadboard HIP.

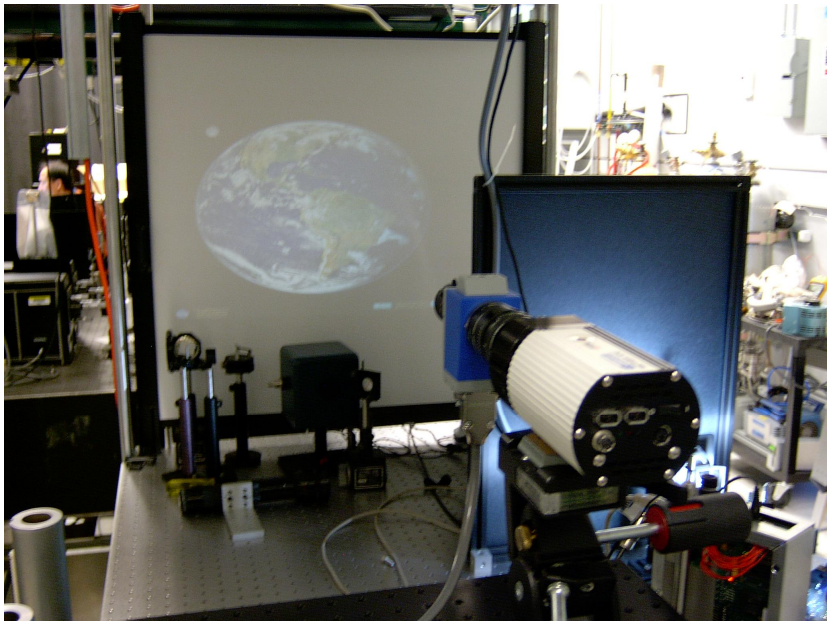

Figure 4. Bench HIP system projecting an Earth-view onto a screen. The reference camera is in the foreground.

We have used a Xe lamp as well as a supercontinuum source in the bench-top HIP. We have experimentally demonstrated the feasibility of this concept in the visible spectral range in previous work, showing that power densities of 1 mW/nm at 1 nm spectral resolution, at spatial resolutions such as 1024 x 768 and better, is feasible.

The reference hyperspectral imager

Validation of system-level performance of the UUT does not require a perfect match between the projected scene and the input hyperspectral data cube. To validate the system-level performance of sensors, the projected scenes need to only approximate realistic scenes that the UUT will see on-orbit; however, the projected scenes must have a known spectral/spatial radiance distribution, with established uncertainties. It is the reference instrument that provides us with knowledge of the scene radiance. The current reference instrument consists of a commercially-available liquid crystal tunable filter (LCTF) in front of a CCD camera. Our LCTF operates from 400 nm to 720 nm with a bandwidth of 7 nm. LCTFs at longer wavelengths are also commercially available. We have developed data acquisition software that automatically tunes the LCTF to each successive band of a contiguous set of monochromatic bands, capturing the image at each band. Thus the reference instrument acts as a staring-mode hyperspectral imager. Tuning times are in the millisecond range. The CCD integration time is variable, depending on the desired signal-to-noise level and the frame rate at which we operate the HIP, which is synchronized to the camera exposure signal. Capturing a full hypercube of, for instance, 42 bands typically takes tens of seconds with such a system. Consequently, it may not be appropriate for real, live, dynamic scenes, since there the spatial image typically changes too much from one band to the next. However, it is indeed a good match with HIP, given that we can control the scene and ensure that it does not change during image cube acquisition.

The reference instrument will be characterized on the NIST SIRCUS facility [8]. Scenes measured by the instrument will be corrected for both spectral and spatial scattered light, based on the SIRCUS characterization, using algorithms developed at NIST. The radiance responsivity will be determined measuring lamp-illuminated integrating spheres traceable to primary national radiometric standards maintained at NIST [15]. Proper development of an uncertainty budget and consistent maintenance of the reference instrument's radiance responsivity is critical to the successful integration of the new test facility into satellite sensor calibration protocols. Prior to validating the system-level performance of hyperspectral sensors with the HIP, a detailed uncertainty budget for the reference hyperspectral imager will be developed, and the uncertainty in a particular scene quantified, following international guidelines [16].

4. DISCUSSION

For a scanning instrument like MODIS, the scene generator can provide stripes at the system level in the along-track direction, that is, narrow bands of light covering all or part of a single band. This duplicates the light from an illuminated slit. However, the color, width, and position of the stripe can be varied without changing the experimental setup, as can its brightness. Each band can be illuminated, either across its full width or in part. The process can be repeated, again without setup changes, for stripes in the cross-track direction. Yet again, the process can be repeated for the illumination of a single detector or group of detectors. These are the basic system-level measurements required to determine the contamination the focal plane output from the illumination of any part of the focal plane. A complete set of measurements can be accomplished in one experimental setup – without the concerns of complications in the results from artifacts from the setup changes.

This set of measurements can be performed at the subassembly level, that is, at the level of the focal plane itself. This requires the incorporation of a fore optic in the test equipment, such as a collimator, to replace the input optics of the instrument. However, for testing by any other means, such a fore optic is also required. Again, the scene generator allows the full set of measurements with one test setup. With a modification to the focal plane, the same tests can be performed with the filters removed. In this manner, the effects of electrical crosstalk can be examined without the effects of optical crosstalk from the filters.

In addition to providing an alternative to the system level illumination of the instrument using a slit, the generator can duplicate illumination as a knife edge is passed across the focal plane. It can replace the simple test patterns, such alternating bright and dark stripes used for testing of the spatial response of the instrument. These include line and point

spread functions, as wall as the modulation transfer function. The full range of instrument testing, currently performed by other types of instrument illumination, can be accomplished by the scene generator. And these tests can be developed off-line, that is, in parallel with the development of the instrument itself. It is important to repeat the idea that the scene generator removes many of the test artifacts derived from the reconfiguration of the test apparatus as the type of instrument test is changed. Such artifacts add ambiguities to the test results, ambiguities that slow down the analysis process and cloud the results. The HIP can be used for the characterization of push broom instruments such as the Advanced Land Imager (ALI), as well as whisk broom instruments such as MODIS.

5. CONCLUSIONS

In conclusion, we have presented the conceptual basis behind a hyperspectral image projector for satellite sensor characterization and performance validation. The same setup can be used to generate simple line spectra for focal plane characterization as well as complex 2-dimensional scenes that mimic scenes that the sensor will see on-orbit. Available spectral power densities of 1 mW/nm at resolutions of 1 nm have been demonstrated. Improved instrument characterization is critical if satellite sensors are to achieve the uncertainty required to support future climate missions. The HIP should be considered in a re-examination of the fundamental protocols of instrument characterization. Before it can be used to characterize a satellite sensor, however, HIP scenes and performance specifications, as well as its radiometric uncertainty budget, need to be developed.

ACKNOWLEDGEMENTS

We would like to acknowledge the guidance and support for this work by Gerald T. Fraser. This work is funded in part by the NIST Advanced Technology Program (ATP) and the NIST Office of Law Enforcement Standards (OLES); B. Myers was supported by the National Science Foundation under Agreement No PHY-045340.

Note: References are made to certain commercially available products in this paper to adequately specify the experimental procedures involved. Such identification does not imply recommendation or endorsement by the National Institute of Standards and Technology, nor does it imply that these products are the best for the purpose specified. DLP and DMD are trademarks of Texas Instruments, Inc.

REFERENCES

1. Korechoff, R. P., D. J. Diner, D. J. Preston, and C. J. Bruegge, "Spectroradiometer focal plane design considerations: Lessons learned from MISR camera testing," *Proc. SPIE* **2583**, 104-116 (1995).
2. Barnes, R. A., A. W. Holmes, and W. E. Esaias, Stray Light in the SeaWiFS Radiometer, NASA TM 104566, Vol. 31, S. B. Hooker, E. R. Firestone, and J. G. Acker, eds., (NASA Goddard Space Flight Center, Greenbelt, MD, 1995).
3. Rice, J. P., S. W. Brown, B. C. Johnson, and J. E. Neira, "Hyperspectral image projectors for radiometric applications," *Metrologia* **43**, S61-S65 (2006).
4. Brown, S. W., J. P. Rice, J. E. Neira, R. Bousquet, and B. C. Johnson, "Hyperspectral image projector for advanced sensor characterization," *Proc SPIE* **6296**, 6296-02 (2006)
5. Rice, J. P., S. W. Brown, and J. E. Neira, "Development of hyperspectral image projectors," *Proc. SPIE* **6297**, 6297-01 (2006).
6. Rice, J. P., S. W. Brown, J. E. Neira, and R. Bousquet, "A hyperspectral image projector for hyperspectral imagers," *Proc. SPIE* **6565**, 6565-11 (2007).
7. http://www.dlp.com.
8. Brown, S. W., Eppeldauer, G. P., and Lykke, K. R., "Facility for spectral irradiance and radiance responsivity calibrations using uniform sources," *Appl. Opt*. **45**, 8218-8237 (2006).
9. Zong, Y., S. W. Brown, B. C. Johnson, K. R. Lykke, and Y. Ohno, "Simple spectral stray light correction method for array spectroradiometers," *Appl. Opt*. **45**, 1111-1119 (2006).
10. Zong, Y., S. W. Brown, K. R. Lykke, and Y. Ohno, "Correction of stray light in spectroradiometers and imaging instruments," CIE Proceedings, Beijing, China (2007).
11. MacKinnon, N., U. Stange, P. Lane, C. MacAulay, and M. Quatrevalet, "Spectrally programmable light engine for in vitro or in vivo molecular imaging and spectroscopy, " *Appl. Opt*. **44**, 2033-2040 (2005).
12. Lara, H. and Eichenholz, J., "Spectral processor and ASE source aid fiber sensing," Laser Focus World, Jan. 2004.

13. Spectrum measured from Fianium SC-450 Optical Supercontinuum System, www.fianium.com.
14. dVision 30 Series projectors, Digital Projection, Inc., Kennesaw, GA.
15. Walker, J. H., R. D. Saunders, and A. T. Hattenburg, NBS Measurement Services: Spectral Radiance Calibrations, Natl. Bur. Stand. (U.S.), Spec. Publ. 250-1 (U. S. Government Printing Office, Washington, DC, 1987).
16. Taylor, B. N. and C. E. Kuyatt, Guidelines for Evaluating and Expressing the Uncertainty of NIST Measurement Results, Nat'l. Inst. Stand. Technol. Tech. Note 1297 (U. S. Government Printing Office, Washington, DC, 1994).